SIMULATION OF SPIN WAVES EXCITATION BY THE IMPACT OF AN ELECTRIC FIELD ON THE DOMAIN WALL IN MAGNETIC FILMS WITH INHOMOGENEOUS MAGNETOELECTRIC INTERACTION

© 2025 N. V. Myasnikov[a,b,] *, A. P. Pyatakov[a,b]

[a]*Faculty of Physics, Lomonosov Moscow State University, Moscow, Russia*

[b]*MIREA - Russian Technological University, Moscow, Russia*

**e-mail: miasnikov.nv16@physics.msu.ru*

Received September 06, 2024

Revised September 16, 2024

Accepted September 30, 2024

Abstract. We simulated the dynamics of electric field impact on the domain wall in magnetic films with inhomogeneous magnetoelectric interaction. The result of the simulation is the fact that both homogeneous electric field and inhomogeneous electric field induce excitation of spin waves.

Keywords: *micromagnetism, inhomogeneous magnetoelectric interaction, spin waves*

DOI: 10.31857/S03676765250122e3

INTRODUCTION

Recently, new branches of electronics such as spintronics[1] and magnonics[2] have been actively developing in the world. Within the framework of spintronics, all possible electronics devices related to magnetic moment control are considered. This control can take the form of spin transfer by creating spin-polarized currents, or the form of switching the magnetic moment by spin-polarized current or electric field. In the field of magnonics, the main subject of study is spin waves, i.e., magnetic moment precession waves. Such waves as an information carrier have a number of advantages: for spin waves as collective excitations of the magnetic sublattice, there is no leakage into the surrounding space that does not have an ordered magnetic structure; short spin waves can contribute to the miniaturization of devices down to the size of a unit cell; even at room temperature, spin waves in garnet ferrite can travel thousands of their lengths . [2]

The control of the magnetic moment by the electric field in ferrimagnets can be realized due to the inhomogeneous magnetoelectric interaction. This interaction, at the microscopic level provided by the Dzyaloshinski-Moria interaction[3, 4, 5] , promotes the appearance of electric polarization[6, 7] at micromagnetic structures in a medium with inhomogeneous magnetization distribution (e.g., domain walls). Since the Dzyaloshinsky-Moriya interaction is an anisotropic correction to the isotropic exchange interaction arising from the spin-orbit interaction, the inhomogeneous magnetoelectric interaction can manifest itself in ferro-, ferri-, and antiferromagnetics. Thus, the domain wall, a transition region between two magnetic domains where the magnetization vector undergoes a reversal, can respond to an external inhomogeneous electric field[8] . Inhomogeneous magnetoelectric interaction also allows the nucleation of cylindrical magnetic domains with 180° and 90° domain wall orientations[9, 10] . An important aspect is that the works [7,8,9] do not use dynamical models to analyze the effects. Modeling the motion of the domain wall in an external electric field is of interest because, on the one hand, it belongs to the field of spintronics and magnetoelectric effect, and on the other hand, the motion of the domain wall in an external electric field can be considered in the framework of magnonics as a way to excite spin waves by analogy with the discussed way of excitation of spin waves by advancing the domain wall in an external magnetic field[11] . In addition, it is known from classical literature that theoretical analysis of the dynamics of domain wall motion is a separate and challenging problem[12, 13] . In this paper, the simplest case of the dynamics of ferromagnetic domain wall motion in an external electric field leading to the excitation of spin waves is investigated theoretically and numerically.

THEORY

The Landau-Lifshitz-Hilbert equation was used to calculate the magnetization dynamics in the micromagnetic approximation:

$$\frac{\partial \vec{m}}{\partial t} = -\gamma\left[\vec{m} \times \vec{H}^{eff}\right] + \alpha\left[\vec{m} \times \frac{\partial \vec{m}}{\partial t}\right], \tag{1}$$

where$\vec{m}$ is the dimensionless vector field of magnetization having at each point a modulus equal to unity,$\vec{H}^{eff}$ is the effective magnetic field,γ is the gyromagnetic ratio for an electron,α is the attenuation index for a given material. In the following, it is understood that the equation ( )1 is used to describe the dynamics of magnetization in a ferromagnetic material characterized by the parameters of garnet ferrite films, which are popular elements in possible magnonics devices[14, 15] , so all parameters of the problem (e.g., saturation magnetizationM_s) characterize (in order of magnitude) exactly garnet ferrite films. Garnet ferrites are ferrimagnets, but the strongest exchange interaction binds two magnetic sublattices in them[12] and makes the magnetic moments of the sublattices collinear in statics. Therefore, we use the static parameters of the garnet ferrite films for clarity. The effective magnetic field is defined as the negative variational derivative of the free energy along the magnetization vector:

$$\vec{H}^{eff} = -\frac{1}{M_s}\frac{\delta F(\vec{m})}{\delta \vec{m}}. \qquad (2)$$

The free energy of the inhomogeneous electric interaction is described by the following expression :[5, 6]

$$F_{me} = -\gamma_{me}\left(\vec{E}\cdot\left(\vec{m}(\nabla\cdot\ \vec{m}) + \left[\vec{m}\times[\nabla\times\vec{m}]\right]\right)\right), \qquad (3)$$

whereγ_{me} is the magnetoelectric constant,$\vec{E}$ is the electric field inside the material given by an external source. In the expression ( )3 the multiplier scalarly multiplied by the electric field vector plays the role of electric polarization induced by inhomogeneous distribution of magnetization. The energyF_{me} corresponds, in agreement with the expression ( )2 , to the effective magnetic field with the following components in the Cartesian coordinate system :[6]

$$\left(\mathrm{H}_{\mathrm{me}}^{\mathrm{eff}}\right)_{\mathrm{i}} = \gamma_{\mathrm{me}}\left(2\mathrm{E}_{\mathrm{i}}\,\partial_{\beta}\mathrm{m}_{\beta}\text{-}2\mathrm{E}_{\beta}\,\partial_{\mathrm{i}}\mathrm{m}_{\beta} + \mathrm{m}_{\beta}\,\partial_{\beta}\mathrm{E}_{\mathrm{i}}\text{-}\mathrm{m}_{\beta}\,\partial_{\mathrm{i}}\mathrm{E}_{\beta}\right). \qquad (4)$$

Since we are talking about the effect of the electric field on the magnetization$\vec{m}$, which is characteristic of the domain wall, we need to set the exchange interaction energy and the magnetic anisotropy energy. The simplest model was chosen for the analysis, in which the following expressions for the energy density of the exchange interaction and magnetic anisotropy, respectively, are valid:

$$F_{ex} = A \sum_{i=\overline{1,3}} (\nabla m_i \cdot \nabla m_i), \quad (5)$$

$$F_{an} = -K_u m_z^2, \quad (6)$$

where$A = 1 \cdot 10^{-7}$ erg/cm is the exchange interaction constant,$K_u = 1000$ erg/cm^{3}is the uniaxial magnetic anisotropy constant. The geometry of the problem is summarized in Fig. 1a. For the sum of energies ( ) , (56), the classical one-dimensional solution is known.

$$m_x = \sin(\theta_w(y)) \cos(\varphi_w), \quad (7)$$

$$m_y = \sin(\theta_w(y)) \sin(\varphi_w), \quad (8)$$

$$m_z = \cos(\theta_w(y)), \quad (9)$$

$$\theta_w(y) = 2\arctan(\exp(y/\Delta_w)), \quad (10)$$

describing the Bloch domain wall[12, 16] at ,$\varphi_w = 0 \varphi_w = \pi$ and the Neel domain wall at ,$\varphi_w = \pi/2 \varphi_w = 3\pi/2$. Here$\Delta_w = \sqrt{A/(K_u + 2\pi M_s^2 (\sin \varphi_w)^2)}$ is the parameter defining the width of the domain wall,φ_w is the angle defining the position of the magnetization in the film plane. Note, firstly, that in the classical Bloch domain wall from the energy point of view the different states with$\varphi_w = 0$ and$\varphi_w = \pi$ are indistinguishable and, secondly, that the Bloch domain wall in statics does not give a contribution to the inhomogeneous magnetoelectric effect, since the expression ( )3 for the structure ( )7 at$\varphi_w = 0$ and$\varphi_w = \pi$ is zero.

Before turning to numerical modeling, we should perform analytical calculations as far as possible. We will consider analytically a one-dimensional domain wall to which homogeneous electric field is applied. It is important to note that the expression

(3) contains the electric field vector, which can be either inhomogeneous or homogeneous. Here, in the analytical consideration, the homogeneous electric field is used in order to keep it possible to draw simple conclusions and compare them with the results of numerical experiment. In the equilibrium state of the domain wall, which is described by the expressions (7) , before the application of the electric field, the total effective magnetic field of the exchange interaction and magnetic anisotropy is zero, so at the first instant of time after the application of the electric field, the domain wall is in the effective field $\vec{H}_{me}^{eff}$. The equation (1) can be written for the angle θ[12, 13] , which determines the position of magnetization with respect to the *Oz* axis (hereinafter it coincides with the normal to the surface of the magnetic film). The effective field (4) leads to the following differential equation for the angle θ , describing the magnetization in an arbitrary domain wall, under a uniform electric field E_x , directed along the Ox axis:

$$\frac{\partial\theta}{\partial t} = -v_{E_x}\frac{\partial\theta}{\partial y}, \tag{11}$$

where $v_{E_x} = 2\gamma\gamma_{me}E_x\cos(\theta)/M_s$. For the case of a homogeneous field E_z the following equation is valid:

$$\frac{\partial\theta}{\partial t} = v_{E_z}\frac{\partial\theta}{\partial y}, \tag{12}$$

where , $v_{E_z} = 2\gamma\gamma_{me}E_z\sin(\theta)\cos(\varphi)/M_s$ φ is the azimuthal angle specifying the position of magnetization in the film plane (see Fig. 1a). Equations (11), (12) belong to the class of transport equations with a known solution of the form $f\big(t - y/v(\theta)\big)$, where $v(\theta)$ is the coefficient on the derivative in the spatial coordinate, which has the velocity dimension. It is important to note that an important conclusion follows from the equation (12) that inhomogeneous magnetoelectric interaction leads to different dynamics of the Bloch domain wall with positive and negative componentsm_x , since the shear ratev_{E_z} is proportional to$\cos(\varphi)$, which at$\varphi = 0, \pi$ sets the magnetization reversal structure. In other words, two Bloch domain walls with different signm_x in a homogeneous electric fieldE_z will move in opposite directions. Fig. 1b shows the dependence of the magnetization vector components on the coordinate in the Bloch domain wall described by expressions (7-10) and the corresponding velocity directions from expressions(11) and (12), communicated to the domain wall by the electric field at the initial moment of time after turning on the electric field. According to (7)-(10)$v_{E_z} \sim m_x$ and has a constant sign along the width of the Bloch domain wall, while$v_{E_x} \sim m_z$ and changes sign along the width of the Bloch domain wall. It follows that the homogeneous electric fieldE_x does not shift the domain wall as a whole, but leads at early stages of dynamics to compression or broadening of the domain wall - depending on the signE_x . At the same time, the homogeneous electric fieldE_z leads in the dynamics to a shift of the Bloch domain wall as a whole. Also from the equation (12) it follows that the Neel ($\varphi = \pi/2, 3\pi/2$) domain wall will not respond to the electric field directed along the normal to the film, but will change its width in the electric fieldE_x like the Bloch domain wall. Strictly speaking, the equations (11), (12) are only applicable at the initial time instant after application of the electric field by the step, because the balance between the magnetic anisotropy and exchange interaction energies is disturbed at subsequent time instants. Therefore, it is necessary to solve the equation ( )1 numerically.

For possible comparison, the dispersion law for low amplitude exchange spin waves propagating in a ferromagnetic material without domain walls should also be given :[17]

$$\omega^2 = (\omega_a + \omega_{ex})\left(\omega_a + \omega_{ex} + \omega_M \frac{k_x^2 + k_y^2}{k^2}\right),$$

$$\omega_{an} = \gamma \frac{2K_u}{M_s},$$

$$\omega_{ex} = \gamma \frac{2A}{M_s} k^2, \quad (13)$$

$$\omega_M = 4\pi\gamma M_s,$$

where$k^2 = k_x^2 + k_y^2 + k_z^2$ is the square of the wave vector modulus,$\omega_{an}, \omega_{ex}, \omega_M$ are the frequencies given by magnetic anisotropy, isotropic exchange interaction, and demagnetization fields, respectively. Thus, the precession frequency is proportional to the square of the wave vector. It should be noted that the expressions (13) are obtained in the approximation of small and constant with time precession amplitude. In the case of$k = 0$ magnetic moments precess synchronously in an effective magnetic field of magnetic anisotropy. This field at the given problem parameters has a value of 500 Å, which corresponds to the frequency of ferromagnetic resonance$\omega_{an}/(2\pi) = 1.4$ GHz.

NUMERICAL CALCULATION METHOD

The numerical solution of the Landau-Lifshitz-Hilbert equation was carried out using the finite element method based on the FEniCS library[18, 19] . In the one-dimensional model there were 30 nodes of the computational grid per segment corresponding to one width of the domain wall $\Delta = \sqrt{A/K_u}$, and 7 nodes in the two-dimensional model. The calculation was performed taking into account the demagnetizing fields: in the case of the one-dimensional model an additional energy term was used $F_M = 2\pi M_s^2 m_y^2$, in the case of the two-dimensional model the structure of the demagnetizing fields was calculated from the Poisson equation for the scalar potential $\Delta u = 4\pi M_s \operatorname{div} \vec{m}$. The calculations were performed with the attenuation coefficient α = 0.0001, M_s = 4 Gs, and electric field strength of 3 MV/cm. The electric field was applied to the system in a step in time. Such a value of the electric field is necessary for the clarity of the results and the possibility to consider the properties of spin waves.

NUMERICAL SIMULATION RESULTS

This section discusses the results of the numerical simulations. Throughout the section, they are compared with the conclusions following from the equations (11), (12), but we are talking about the numerical solution of the Landau-Lifshitz-Hilbert equation (1) and the graphical representation of this solution. In the one-dimensional model based on the equation (1) with initial condition (7)-(10), the dependence of the magnetization vector in the Bloch domain wall on time was obtained. The calculation results for different direction of homogeneous electric field are shown in Fig. 2. When an electric field E_z is applied, the domain wall shifts to the right (Fig. 2a) from its initial state (Fig. 2b) in a time of 565 ps, in accordance with the conclusion following from the equation (12) , while spin waves appear along the course of the domain wall motion. In addition, when the sign of the m_x component in the initial state of the domain wall is changed to the opposite sign over the same time period, the Bloch domain wall shifts in the opposite direction (Fig. 2c) When an electric field$-E_x$ is applied over a time period of 847.5 ps, the domain wall as a whole does not experience a shift (Fig. 2d), as follows from the equation (11) , but spin waves occur to the left and right of the domain wall. The Neel domain wall, stabilized by an external magnetic field exceeding the demagnetization field by a factor of two, experiences similar dynamics when an electric field$-E_x$ is applied - it remains in place as a whole, but spin waves appear at the periphery (Fig. 3a,b). At the same time, the numerical calculation shows that the Neel domain wall does not respond to a homogeneous electric fieldE_z (Fig. 3c), as argued in the previous section.

In order to analyze the properties of spin waves excited in this way, a fragment of the dependence ofm_y (for the Bloch wall) andm_x (for the Neel wall) on coordinates and time, containing several wavelengths, was selected for each direction of the electric field. For the Neel domain wall, such a fragment is shown in Fig. 3г. In Fig. 3d shows the dependence of the modulus of the amplitude of the spectrum of the$m_x(t, y)$ function in time on the frequency and coordinates of the fragment. This dependence shows that the characteristic frequency of spin waves in the case of the Neel domain wall and electric field$-E_x$ is 7.5 GHz. Also in Fig. 3d it can be seen that the precession frequency increases with increasing coordinate. This can be explained by the fact that the nonlinearity of the dynamics leads to the fact that the magnetization precession is not isochronous, i.e., the precession frequency depends on its amplitude. We can identify at least one factor that sets the character of this relation. At this site, the strongest effective magnetic field that sets the precession properties of the planar components of magnetization is created by magnetic anisotropy. This effective field, as follows from (2) and (6), is proportional to m_z . Since in Fig. 3d with distance from the domain wall the amplitude of the planar components m_x, m_y naturally decreases, the component m_z grows, and consequently a larger effective magnetic field sets a higher precession frequency. Of course, for the model under consideration, such a consideration is very simple, but it shows that the increase in the frequency of spin waves with distance from the domain wall is not unexpected. A more rigorous consideration in perspective can be obtained by analyzing the influence of all interactions on the dispersion relation for spin waves. In Fig. 3e shows the dependence of the modulus of the spectrum of the function $m_x(t, y)$ in spatial coordinate on the spatial frequency for the time instant $t = 565$ ps. This dependence shows that the characteristic spin wavelength is 500 nm. Similarly, the fragments of Fig. 1, highlighted by blue filling, were selected for the Bloch domain wall. For the cases of homogeneous electric field E_z and -E_x , applied to the Bloch domain wall, the characteristic frequencies and wavelengths are 15 GHz, 200 nm and 7.5 GHz, 500 nm, respectively.

In the two-dimensional model, spin waves are also excited under the electric field of a point charge. Fig. 4a shows the initial state of the Bloch domain wall and the position of the point charge. In a time of 170 ps after application of an electric field in a stepwise manner, the domain wall curves and shifts (Fig. 4b). In this case, the electric field component along the *Oz* axis has a negative sign and the m_x component has a positive sign ($\cos(\varphi) > 0$). In this configuration, equation (12) describes the direction of the domain wall displacement corresponding to Fig. 4b. The electric field causes, in addition to the domain wall shift, the excitation of spin waves, which are reflected in the distribution of them_x component in Fig. 4b. and in the distribution of the components ,$m_x m_y$ (Fig. 4c) plotted along the specific direction marked in Fig. 4b. In Fig. 4d shows the spectrum of them_y component over time for each point in the fragment. It follows that the characteristic frequency of the excited spin waves is 12.5 GHz. The spatial spectrum in Fig. 4d shows that the characteristic spin wavelength in the two-dimensional model is 300 nm.

CONCLUSION

Thus, using micromagnetic modeling based on the Landau-Lifshitz-Hilbert equation for ferromagnetic material, it is shown that in films with inhomogeneous magnetoelectric interaction, the effect of both homogeneous and inhomogeneous electric field on the Bloch and Neel domain walls leads to the excitation of spin waves with characteristic frequencies of about 10 GHz and wavelengths of about 100 nm. The obtained set of pairs of frequencies and wavelengths (15 GHz, 200 nm), (7.5 GHz, 500 nm), (12.5 GHz, 300 nm) qualitatively satisfies the dispersion relation (13) : the smaller the wavelength, the larger the frequency. It is also shown that on the basis of approximate transport equations (11), (12) it is possible to make a conclusion about the presence or absence of the domain wall shift, about the connection of its sign with the polarity of the electric field and the structure of the domain wall. Here it is important to note that in contrast to the static model, the dynamic model admits the possibility of electric field influence on the Bloch domain wall. These conclusions imply further experimental work on the detection of spin waves, checking the relationship between the direction of the electric field and the shear properties of the domain wall. From the theoretical point of view, an important question is the effect of the electric field on the dispersion relation for excited spin waves, as well as the question of the dependence of the properties of spin waves on the amplitude of the electric field. There is also a question about the applicability of the results of the work to the case of ferrimagnetic materials. It is known[12] that two types of precession of magnetic moments of two sublattices are possible in ferrimagnetics: low-frequency (characteristic frequencies are comparable to those of ferromagnetics), when magnetic moments of sublattices remain collinear, and high-frequency, when collinearity is broken. The second type of precession allows ferrimagnetics to be used to excite spin waves in the terahertz range[2] . In the case of garnet ferrite films, the exchange interaction between the sublattices is the strongest, while the Dzyaloshinski-Moria interaction is of a corrective nature due to the smallness of the spin-orbit interaction constant. Therefore, at low applied electric fields, the inhomogeneous magnetoelectric interaction will not be able to break the collinearity of magnetic sublattices and excite high-frequency waves. To estimate the smallness of the electric field, we can indicate that at an electric field value of 1 MV/cm, the magnitude of the inhomogeneous magnetoelectric interaction is a few tens of percent of the surface energy of the domain wall[10] , and, accordingly, an even smaller percentage of the exchange energy. Therefore, at electric field values smaller than 1 MV/cm, one should not expect a violation of the collinearity of magnetic sublattices in a ferrimagnet. In order to determine the specific precession parameters and to verify the above hypothesis, it is necessary to carry out appropriate modeling. In the case of antiferromagnetics with more than two magnetic sublattices, a separate calculation is required.

FUNDING

This work was supported by the BASIS Foundation for the Development of Theoretical Physics and Mathematics (Grant№ 22-1-2-49 "Young Leading Scientist (Theoretical Physics)") and by the Ministry of Science and Higher Education of the Russian Federation (Grant No. 075-15-2022-1131).

REFERENCES

1. *Bader S.D., Parkin S.S.P.* // Ann. Rev. Cond. Matter Phys. 2010. V. 1. No. 1. P. 71.
2. *Barman A., Gubbiotti G., Ladak S. et al.* // J. Phys. Phys. Cond. Matter. 2021. V. 33. Art. No. 413001.
3. *Dzyaloshinsky I.E.* // ZhETF. 1957. T. 32. №. 6. C. 1547.
4. *Moriya T.* // Phys. Rev. 1959. V. 120. No. 1. P. 91.
5. *Zvezdin A.K., Pyatakov A.P.* // EPL. 2012. V. 99. No. 5. P. 57003.
6. *Pyatakov A.P., Meshkov G.A., Zvezdin A.K..* // J. Magn. Magn. Mater. 2012. V. 324. No. 21. P. 3551.
7. *Chomsky D.I.* // Letters in ZhETF. 2021. T. 159. № 4. C. 581; *Khomskii D.I.* // JETP Lett. 2021. V. 132. No. 4. P. 482.
8. *Logginov A.S., Meshkov G.A., Nikolaev A.V., Pyatakov A.P.* // JETP Lett. 2007. V. 86. P. 115.
9. *Kulikova D.P., Gareev T.T., Nikolaeva E.P. et al.* // Phys. Stat. Sol. (RRL). 2018. V. 12. Art. No. 1800066.

10. *Antipin K.S., Gareev T.T., Myasnikov N.V. et. al.* // J. Appl. Phys. Appl. Phys. 2021. V. 129. No. 2. Art. No. 24103.

11. *Yan M., Andreas C., Ká kay A. et al.* // Appl. Phys. Lett. 2011. V. 99. Art. No. 122505.

12. *Bokov V.A.* Physics of Magnetics. SPb.: Nevsky Dialect, 2002. 272 c.

13. *Malozemov A., Slonzuski J.* Domain walls in materials with cylindrical magnetic domains. M.: Mir, 1982. 382 c.

14. *Sadovnikov A.V., Nikitov S.A.* // Bull. Russ. Acad. Sci. Phys. 2021. V. 85. No. 6. P. 595.

15. *Gubanov V.A., Kruglyak V.V., Sadovnikov A.V.* // Bull. Russ. Acad. Sci. Phys. 2023. V. 87. No. 6. P. 362.

16. *Landau L.D., Lifshits E.M.* Theoretical Physics. T. 8. Electrodynamics of continuous media. Moscow: Fizmatlit, 2016. 656 c.

17. *Shavrov V.G., Shcheglov V.I.* Dynamics of magnetization under conditions of its orientation change. Moscow: Fizmatlit, 2019. 472 c.

18. https://fenicsproject.org.

19. *Abert C., Exl L., Bruckner F. et al.* // J. Magn. Magn. Magn. Mater. 2013. V. 345. P. 29.

FIGURE CAPTIONS

Fig. 1. Geometry of the problem and structure of the Bloch domain wall: geometry of the problem with marked magnetization componentsm_x, m_y, m_z and anglesθ, φ , defining the normalized magnetization vector (a); structure of the Bloch domain wall (b): lines mark the dependence of the magnetization vector components on the coordinate; arrows mark the velocities imparted by the homogeneous electric field (E_x orE_z) to the domain wall at the first moment of dynamics. The coordinate is counted in units of the domain wall width$\Delta = \sqrt{A/K_u} = 100$ nm.

Fig. 2. Numerical simulation result of the Bloch domain wall: initial state (a); with an initially negative componentm_x through$t = 565$ ps at a homogeneous fieldE_z (b); with an initially positive componentm_x through$t = 565$ ps at a homogeneous fieldE_z (c); through$t = 847.5$ ps at a homogeneous field$-E_x$ (d). The coordinate is counted in units of domain wall width$\Delta = \sqrt{A/K_u} = 100$ nm. Blue fillings show the regions selected for calculating the spectral characteristics.

Fig. 3. Result of numerical modeling of the Neel domain wall: initial state (a); structure at the time$t = 565$ ps after application of a uniform electric field$-E_x$ (b), blue fill shows the region selected for calculating spectral characteristics; structure that does not respond to a uniform electric fieldE_z (numerical calculation) (c), upper indices indicate initial and final states; magnetization componentm_x at the time$t = 565$ ps in the selected region (d); time dependence of the function spectrum$m_x(t, y)$ for each

coordinate of the fragment (e); function spectrum $m_x(y)$ by coordinate at the time $t =$ 565 ps (f).

Fig. 4. Two-dimensional numerical modeling of spin waves excitation by electric field: dependence of the m_x component in the Bloch domain wall on the coordinates at the initial time instant and the position of the point electric charge shown by the shaded circle (a); dependence of the m_x component in the Bloch domain wall on the coordinates at time $t =$ 170 ps (b); dependence of the in-plane magnetization components on the coordinate along the line marked in figure b at the moment of time $t =$ 170 ps (c); spectrum of the function $m_y(t, y)$ on time for each coordinate of the fragment (d); spectrum of the function $m_y(r)$ on coordinate at the moment of time $t =$ 170 ps (e).

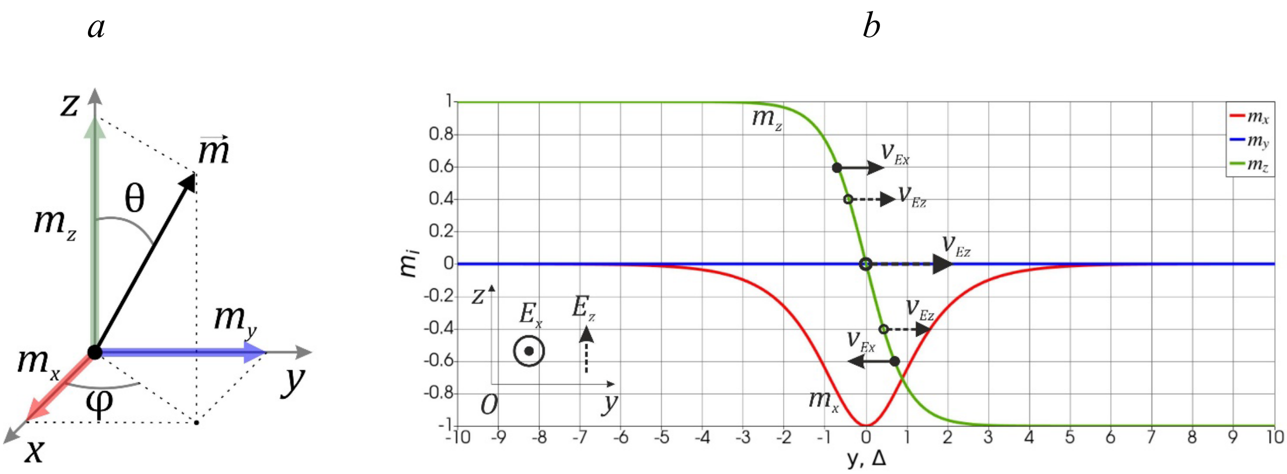

Fig. 1.

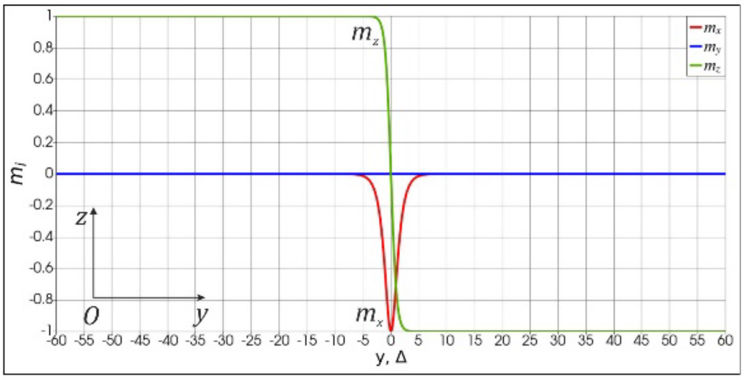
m_i
y, Δ
m_z
m_x
m_y
z
O
y

а

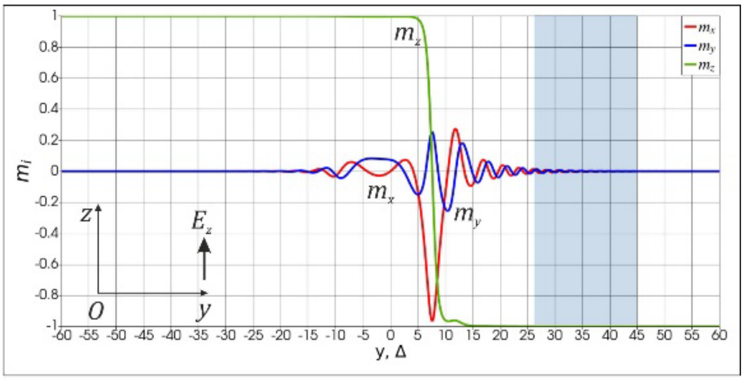
m_i
y, Δ
m_z
m_x
m_y
z
O
y
E_z

б

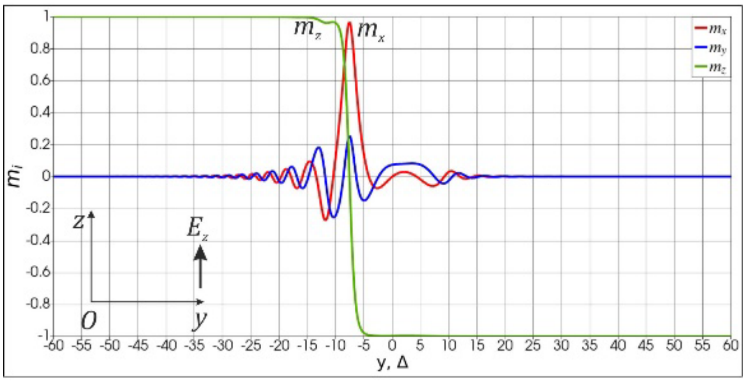
m_i
y, Δ
m_z
m_x
m_y
z
O
y
E_z

в

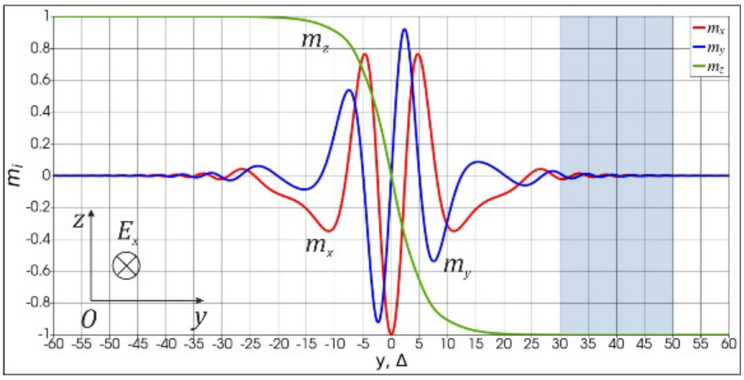
m_i
y, Δ
m_z
m_x
m_y
z
O
y
E_x

г

Fig. 2

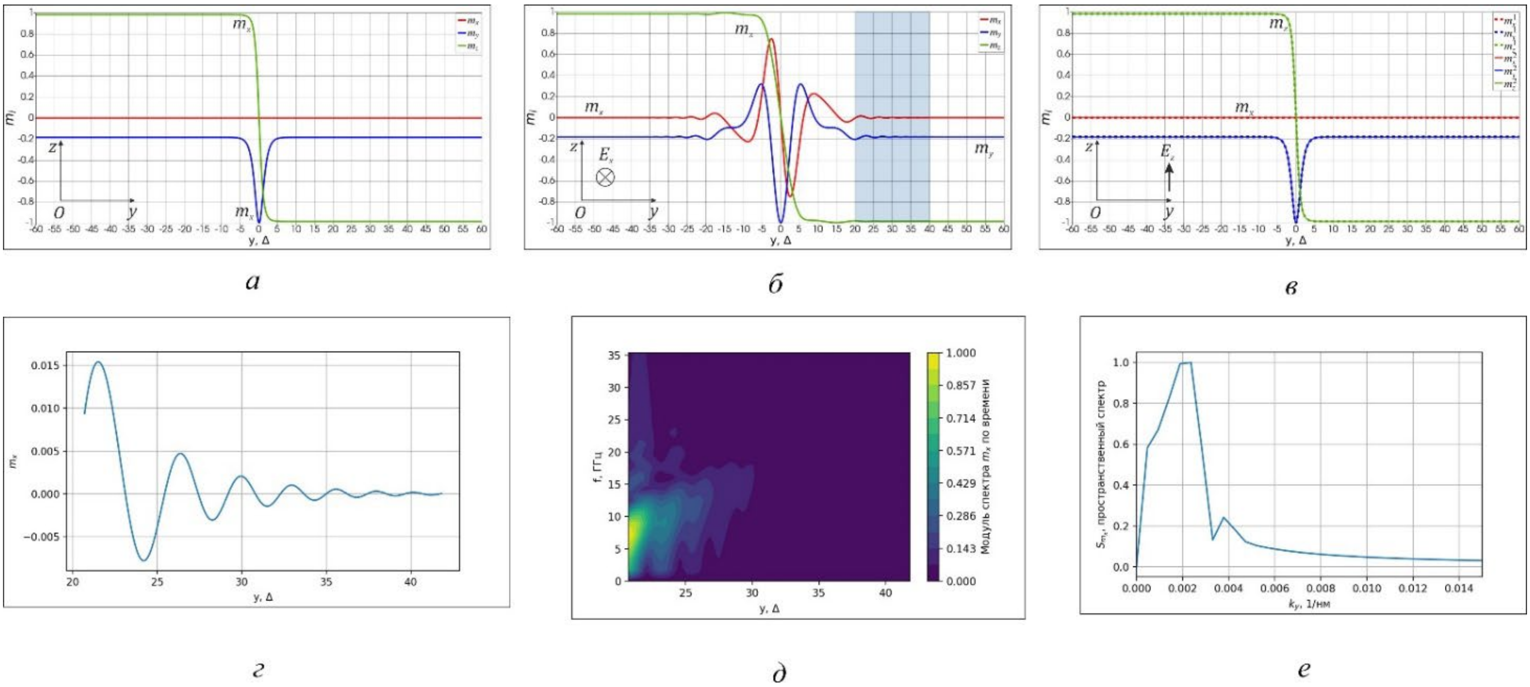

Fig. 3

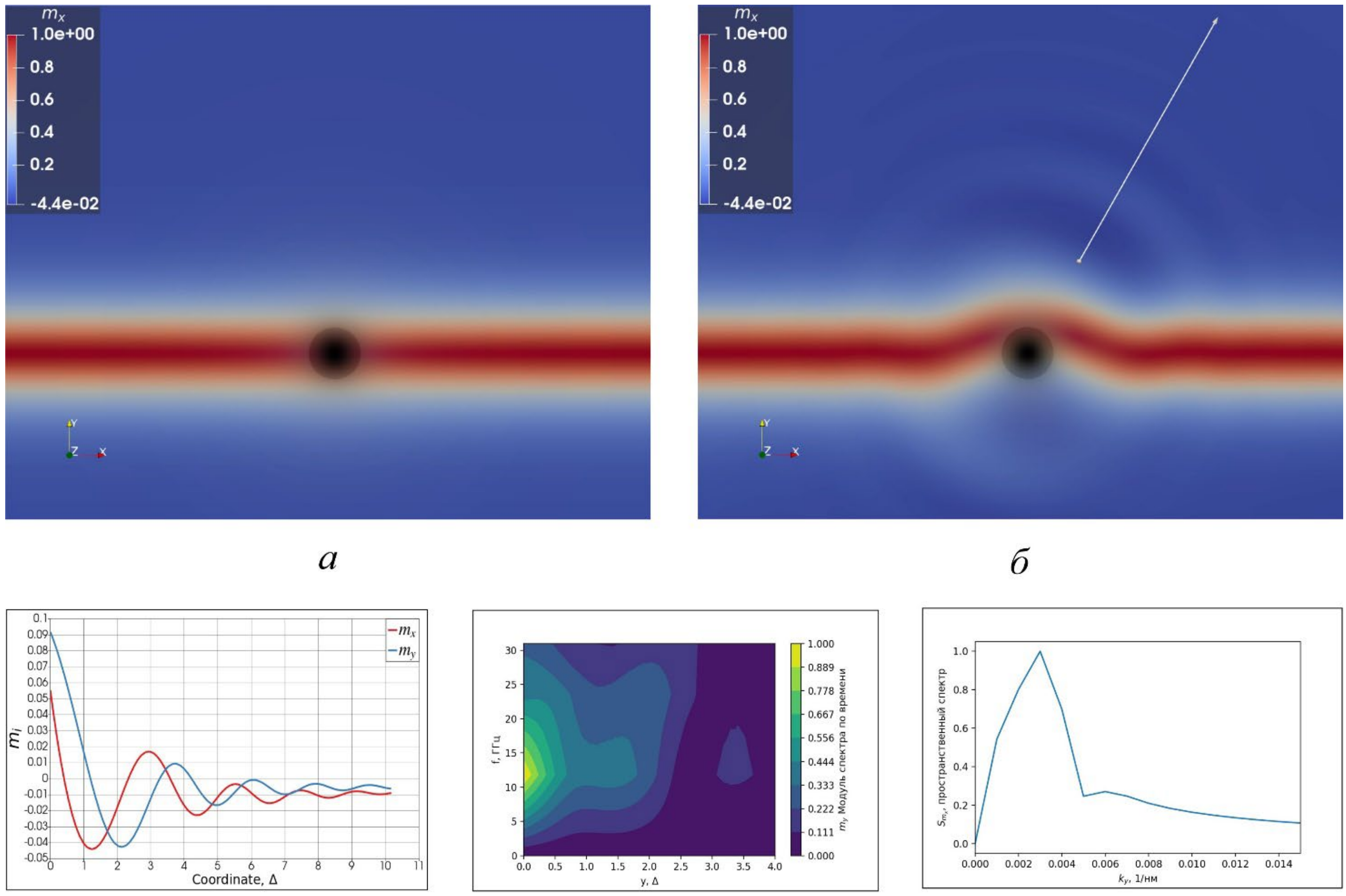
m_x
1.0e+00
0.8
0.6
0.4
0.2
-4.4e-02
m_x
1.0e+00
0.8
0.6
0.4
0.2
-4.4e-02
m_i
m_x
m_y
Coordinate, Δ
f, ГГц
y, Δ
m_y Модуль спектра по времени
S_{m_y}, пространственный спектр
k_y, 1/нм

а *б*

в *г* *д*

Fig. 4